effects of weakly excited beams, replaces the Fourier coefficients of potential by the 'Bethe potentials'

$$U_{\mathbf{h}} = V_{\mathbf{h}} - 2k_0\sigma \sum_{\mathbf{g}} \frac{V_{\mathbf{g}} \cdot V_{\mathbf{h}-\mathbf{g}}}{\kappa^2 - k_{\mathbf{g}}^2}. \qquad (2.5.2.17)$$

Use of these potentials has been shown to account well for the deviations of powder-pattern intensities from the predictions of two-beam theory (Horstmann & Meyer, 1965) and to predict accurately the extinctions of Kikuchi lines at particular accelerating voltages due to relativistic effects (Watanabe *et al.*, 1968), but they give incorrect results for the small-thickness limit.

2.5.2.5. *Kinematical diffraction formulae*

(1) *Comparison with X-ray diffraction.* The relations of real-space and reciprocal-space functions are analogous to those for X-ray diffraction [see equations (2.5.2.2), (2.5.2.10) and (2.5.2.15)]. For diffraction by crystals

$$\varphi(\mathbf{r}) = \sum_{\mathbf{h}} V_{\mathbf{h}} \exp\{-2\pi i \mathbf{h}\cdot\mathbf{r}\},$$

$$V_{\mathbf{h}} = \int \varphi(\mathbf{r}) \exp\{2\varphi i \mathbf{h}\cdot\mathbf{r}\}\, \mathrm{d}\mathbf{r} \qquad (2.5.2.18)$$

$$= \frac{1}{\Omega}\sum_i f_i(\mathbf{h}) \exp\{2\pi i \mathbf{h}\cdot\mathbf{r}_i\}, \qquad (2.5.2.19)$$

where the integral of (2.5.2.18) and the summation of (2.5.2.19) are taken over one unit cell of volume (see Dawson *et al.*, 1974).

Important differences from the X-ray case arise because

(*a*) the wavelength is relatively small so that the Ewald-sphere curvature is small in the reciprocal-space region of appreciable scattering amplitude;

(*b*) the dimensions of the single-crystal regions giving appreciable scattering amplitudes are small so that the 'shape transform' regions of scattering power around the reciprocal-lattice points are relatively large;

(*c*) the spread of wavelengths is small (10^{-5} or less, with no white-radiation background) and the degree of collimation is better (10^{-4} to 10^{-6}) than for conventional X-ray sources.

As a consequence of these factors, single-crystal diffraction patterns may show many simultaneous reflections, representing almost-planar sections of reciprocal space, and may show fine structure or intensity variations reflecting the crystal dimensions and shape.

(2) Kinematical diffraction-pattern intensities are calculated in a manner analogous to that for X-rays except that

(*a*) no polarization factor is included because of the small-angle scattering conditions;

(*b*) integration over regions of scattering power around reciprocal-lattice points cannot be assumed unless appropriate experimental conditions are ensured.

For a thin, flat, lamellar crystal of thickness H, the observed intensity is

$$I_{\mathbf{h}}/I_{\mathbf{0}} = |\sigma(V_{\mathbf{h}}/\Omega)(\sin\pi\zeta_{\mathbf{h}}H)/(\pi\zeta_{\mathbf{h}})|^2, \qquad (2.5.2.20)$$

where $\zeta_{\mathbf{h}}$ is the excitation error for the $\mathbf{h}$ reflection and Ω is the unit-cell volume.

For a single-crystal diffraction pattern obtained by rotating a crystal or from a uniformly bent crystal or for a mosaic crystal with a uniform distribution of orientations, the intensity is

$$I_{\mathbf{h}} = I_{\mathbf{0}} \frac{\sigma^2 |V_{\mathbf{h}}|^2 V_c d_{\mathbf{h}}}{4\pi^2\Omega^2}, \qquad (2.5.2.21)$$

where V_c is the crystal volume and $d_{\mathbf{h}}$ is the lattice-plane spacing.

For a polycrystalline sample of randomly oriented small crystals, the intensity per unit length of the diffraction ring is

$$I_{\mathbf{h}} = I_{\mathbf{0}} \frac{\sigma^2 |V_{\mathbf{h}}|^2 V_c d_{\mathbf{h}}^2 M_{\mathbf{h}}}{8\pi^2\Omega^2 L\lambda}, \qquad (2.5.2.22)$$

where $M_{\mathbf{h}}$ is the multiplicity factor for the $\mathbf{h}$ reflection and L is the camera length, or the distance from the specimen to the detector plane. The special cases of 'oblique texture' patterns from powder patterns having preferred orientations are treated in *IT* C (1999, Section 4.3.5).

(3) *Two-beam dynamical diffraction formulae: complex potentials including absorption.* In the two-beam dynamical diffraction approximation, the intensities of the directly transmitted and diffracted beams for transmission through a crystal of thickness H, in the absence of absorption, are

$$I_{\mathbf{0}} = (1+w^2)^{-1}\left[w^2 + \cos^2\left\{\frac{\pi H(1+w^2)^{1/2}}{\xi_{\mathbf{h}}}\right\}\right] \qquad (2.5.2.23)$$

$$I_{\mathbf{h}} = (1+w^2)^{-1}\sin^2\left\{\frac{\pi H(1+w^2)^{1/2}}{\xi_{\mathbf{h}}}\right\}, \qquad (2.5.2.24)$$

where $\xi_{\mathbf{h}}$ is the extinction distance, $\xi_{\mathbf{h}} = (2\sigma|V_{\mathbf{h}}|)^{-1}$, and

$$w = \xi_{\mathbf{h}}\zeta_{\mathbf{h}} = \Delta\theta/(2\sigma|V_{\mathbf{h}}|d_{\mathbf{h}}), \qquad (2.5.2.25)$$

where $\Delta\theta$ is the deviation from the Bragg angle.

For the case that $\zeta_{\mathbf{h}} = 0$, with the incident beam at the Bragg angle, this reduces to the simple *Pendellösung* expression

$$I_{\mathbf{h}} = 1 - I_{\mathbf{0}} = \sin^2\{2\pi\sigma|V_{\mathbf{h}}|H\}. \qquad (2.5.2.26)$$

The effects on the elastic Bragg scattering amplitudes of the inelastic or diffuse scattering may be introduced by adding an out-of-phase component to the structure amplitudes, so that for a centrosymmetric crystal, $V_{\mathbf{h}}$ becomes complex by addition of an imaginary component. Alternatively, an absorption function $\mu(\mathbf{r})$, having Fourier coefficients $\mu_{\mathbf{h}}$, may be postulated so that $\sigma V_{\mathbf{h}}$ is replaced by $\sigma V_{\mathbf{h}} + i\mu_{\mathbf{h}}$. The $\mu_{\mathbf{h}}$ are known as phenomenological absorption coefficients and their validity in many-beam diffraction has been demonstrated by, for example, Rez (1978).

The magnitudes $\mu_{\mathbf{h}}$ depend on the nature of the experiment and the extent to which the various inelastically or diffusely scattered electrons are included in the measurements being made. If measurements are made of purely elastic scattering intensities for Bragg reflections or of image intensity variations due to the interaction of the sharp Bragg reflections only, the main contributions to the absorption coefficients are as follows (Radi, 1970):

(*a*) from plasmon and single-electron excitations, μ_0 is of the order of 0.1 $V_{\mathbf{0}}$ and $\mu_{\mathbf{h}}$, for $\mathbf{h} \neq 0$, is negligibly small;

(*b*) from thermal diffuse scattering; $\mu_{\mathbf{h}}$ is of the order of 0.1 $V_{\mathbf{h}}$ and decreasing more slowly than $V_{\mathbf{h}}$ with scattering angle.

Including absorption effects in (2.5.2.26) for the case $\zeta_{\mathbf{h}} = 0$ gives

$$\begin{aligned} I_{\mathbf{0}} &= \tfrac{1}{2}\exp\{-\mu_0 H\}[\cosh\mu_{\mathbf{h}}H + \cos(2\pi\sigma V_{\mathbf{h}}H)], \\ I_{\mathbf{h}} &= \tfrac{1}{2}\exp\{-\mu_0 H\}[\cosh\mu_{\mathbf{h}}H - \cos(2\pi\sigma V_{\mathbf{h}}H)]. \end{aligned} \qquad (2.5.2.27)$$

The Borrmann effect is not very pronounced for electrons because $\mu_{\mathbf{h}} \ll \mu_{\mathbf{0}}$, but can be important for the imaging of defects in thick crystals (Hirsch *et al.*, 1965; Hashimoto *et al.*, 1961).

Attempts to obtain analytical solutions for the dynamical diffraction equations for more than two beams have met with few successes. There are some situations of high symmetry, with incident beams in exact zone-axis orientations, for which the many-beam solution can closely approach equivalent two- or three-beam

behaviour (Fukuhara, 1966). Explicit solutions for the three-beam case, which displays some aspects of many-beam character, have been obtained (Gjønnes & Høier, 1971; Hurley & Moodie, 1980).

2.5.2.6. *Imaging with electrons*

Electron optics. Electrons may be focused by use of axially symmetric magnetic fields produced by electromagnetic lenses. The focal length of such a lens used as a projector lens (focal points outside the lens field) is given by

$$f_p^{-1} = \frac{e}{8mW_r} \int_{-\infty}^{\infty} H_z^2(z)\, \mathrm{d}z, \qquad (2.5.2.28)$$

where W_r is the relativistically corrected accelerating voltage and H_z is the z component of the magnetic field. An expression in terms of experimental constants was given by Liebman (1955) as

$$\frac{1}{f} = \frac{A_0(NI)^2}{W_r(S+D)}, \qquad (2.5.2.29)$$

where A_0 is a constant, NI is the number of ampere turns of the lens winding, S is the length of the gap between the magnet pole pieces and D is the bore of the pole pieces.

Lenses of this type have irreducible aberrations, the most important of which for the paraxial conditions of electron microscopy is the third-order spherical aberration, coefficient C_s, giving a variation of focal length of $C_s\alpha^2$ for a beam at an angle α to the axis. Chromatic aberration, coefficient C_c, gives a spread of focal lengths

$$\Delta f = C_c\left(\frac{\Delta W_0}{W_0} + 2\frac{\Delta I}{I}\right) \qquad (2.5.2.30)$$

for variations ΔW_0 and ΔI of the accelerating voltage and lens currents, respectively.

The objective lens of an electron microscope is the critical lens for the determination of image resolution and contrast. The action of this lens in a conventional transmission electron microscope (TEM) is described by use of the Abbe theory for coherent incident illumination transmitted through the object to produce a wavefunction $\psi_0(xy)$ (see Fig. 2.5.2.2).

The amplitude distribution in the back focal plane of the objective lens is written

$$\Psi_0(u,v)\cdot T(u,v), \qquad (2.5.2.31)$$

where $\Psi_0(u,v)$ is the Fourier transform of $\psi_0(x,y)$ and $T(u,v)$ is the transfer function of the lens, consisting of an aperture function

$$A(u,v) = \begin{cases} 1 & \text{for } (u^2+v^2)^{1/2} \le A \\ 0 & \text{elsewhere} \end{cases} \qquad (2.5.2.32)$$

and a phase function $\exp\{i\chi(u,v)\}$ where the phase perturbation $\chi(uv)$ due to lens defocus Δf and aberrations is usually approximated as

$$\chi(uv) = \pi\cdot\Delta f\cdot\lambda(u^2+v^2) + \frac{\pi}{2}C_s\lambda^3(u^2+v^2)^2, \qquad (2.5.2.33)$$

and u, v are the reciprocal-space variables related to the scattering angles φ_x, φ_y by

$$u = (\sin\varphi_x)/\lambda,$$
$$v = (\sin\varphi_y)/\lambda.$$

The image amplitude distribution, referred to the object coordinates, is given by Fourier transform of (2.5.2.31) as

$$\psi(xy) = \psi_0(xy) * t(xy), \qquad (2.5.2.34)$$

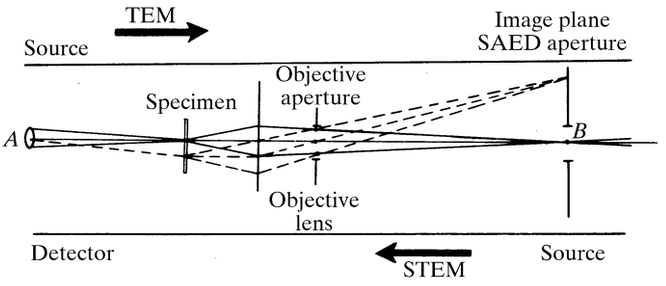

Fig. 2.5.2.2. Diagram representing the critical components of a conventional transmission electron microscope (TEM) and a scanning transmission electron microscope (STEM). For the TEM, electrons from a source A illuminate the specimen and the objective lens forms an image of the transmitted electrons on the image plane, B. For the STEM, a source at B is imaged by the objective lens to form a small probe on the specimen and some part of the transmitted beam is collected by a detector at A.

where $t(xy)$, given by Fourier transform of $T(u,v)$, is the spread function. The image intensity is then

$$I(xy) = |\psi(xy)|^2 = |\psi_0(xy) * t(xy)|^2. \qquad (2.5.2.35)$$

In practice the coherent imaging theory provides a good approximation but limitations of the coherence of the illumination have appreciable effects under high-resolution imaging conditions.

The variation of focal lengths according to (2.5.2.30) is described by a function $G(\Delta f)$. Illumination from a finite incoherent source gives a distribution of incident-beam angles $H(u_1,v_1)$. Then the image intensity is found by integrating incoherently over Δf and u_1, v_1:

$$I(xy) = \int\int G(\Delta f)\cdot H(u_1v_1) \times |\mathscr{F}\{\Psi_0(u-u_1, v-v_1)\cdot T_{\Delta f}(u,v)\}|^2\, \mathrm{d}(\Delta f)\cdot\, \mathrm{d}u_1\, \mathrm{d}v_1, \qquad (2.5.2.36)$$

where $\mathscr{F}$ denotes the Fourier-transform operation.

In the scanning transmission electron microscope (STEM), the objective lens focuses a small bright source of electrons on the object and directly transmitted or scattered electrons are detected to form an image as the incident beam is scanned over the object (see Fig. 2.5.2.2). Ideally the image amplitude can be related to that of the conventional transmission electron microscope by use of the 'reciprocity relationship' which refers to point sources and detectors for scalar radiation in scalar fields with elastic scattering processes only. It may be stated: 'The amplitude at a point B due to a point source at A is identical to that which would be produced at A for the identical source placed at B'.

For an axial point source, the amplitude distribution produced by the objective lens on the specimen is

$$\mathscr{F}[T(u,v)] = t(xy). \qquad (2.5.2.37)$$

If this is translated by the scan to X, Y, the transmitted wave is

$$\psi_0(xy) = q(xy)\cdot t(x-X, y-Y). \qquad (2.5.2.38)$$

The amplitude on the plane of observation following the specimen is then

$$\Psi(uv) = Q(u,v) * \{T(uv)\exp[2\pi i(uX+vY)]\}, \qquad (2.5.2.39)$$

and the image signal produced by a detector having a sensitivity function $H(u, v)$ is

references